Model of the Wind Field in a Downburst

Shangxiang Zhu* and Bernard Etkin†
University of Toronto, Toronto, Canada

The downburst weather phenomenon produces a flow like that of a jet directed vertically downward at the ground. The resulting velocity field near the ground has been modeled as a classical ideal fluid flow generated by a suitable singularity distribution. The resulting model of horizontal, lateral, and vertical winds near the ground is quite realistic, and very useful for investigating landing and takeoff of airplanes under downburst conditions. It can be used both for analysis and on-line real-time simulations.

Nomenclature

D = diameter of a circular doublet sheet
F_B = axes fixed to the airplane
F_W = an Earth-fixed frame—the origin "o" is the point on the ground under the downburst cell's center; "ox" is horizontal and points in the forward direction of the landing airplane
H = height above ground
r = position vector
R_0 = radius of doublet sheet
(u, v, w) = components of airspeed V in F_B
(V_x, V_y, V_z) or (W_1, W_2, W_3) = components of wind speed due to downburst in the reference frame F_W
(x, y, z) = coordinates of a point P in F_W
γ_G = glide slope angle with respect to the horizontal
(ξ, η, ζ) = coordinates of a singularity
$\sigma(r)$ = strength of a doublet sheet

Introduction

THE thunderstorm, with its intense turbulent wind, is one of the more destructive of natural phenomena and has always been dangerous for aviation. It is only recently, however, that thunderstorms have come to be identified with strong, local, highly variable winds near the ground, now known as "downbursts," that present serious hazards to takeoff and landing operations. Downbursts have also been observed on the high plains in the U.S.A. under dry surface conditions.

A 1977 FAA file search revealed the presence or potential of low-level wind shear as a factor in many accidents involving large aircraft, 25 being identified for the period 1964-75. It is significant that in all 25 accidents there was precipitation in the area and in 13 of them there was thunderstorm activity. The weather conditions in these cases are consistent with those with which the downburst phenomenon has been associated.

The catastrophic JFK Airport accident in June of 1975 and others led to examination of aircraft performance in a thunderstorm near the ground. During the course of the investigation of the JFK disaster, T. T. Fujita described a previously undidentified weather phenomenon associated with thunderstorms.[1] He noted that there could be a strong temporary localized downdraft with a speed of up to 30 m/s that hits the ground and spreads horizontally in a radial burst of wind. He suggested that the JFK accident could have been caused by a series of such downbursts bombarding the approach to the runway. Fujita found that some downflows would spread horizontally within a layer only 15 ~ 30 m above the ground and had a diameter of only 3 km—a size that could fit onto an airport. He then coined a new term, "microburst," for a downburst of less than 5.0 km across. Recent research has confirmed the occurrence, nature, and severity of this phenomenon.[2-4]

The effect of microbursts on aircraft performance is a subject of great current interest. To study such effects a model of the wind field is required, and a number of modeling techniques have been used.[5-7] In flight simulators, equations of motion are being run typically at 10-30 iterations/s. This rate imposes limitations on the sophistication of the wind model that can be used. The FAA Rule 14 CFR, Pts. 61 and 121, will allow the simulator to be used for certification checks. This rule requires a large number of meteorological inputs to the simulator; particularly, three-dimensional wind data with time variation are required for adequate training in storm avoidance and storm penetration.

In one recent FAA report,[8] seven candidate standard wind shear profiles for systems qualifications are reported. These models are not truly three-dimensional wind shear. They were constructed from data measured with instrumented towers, from reconstruction of winds from accident flight data records, and from meteorological mathematical models. Among those models, even in so-called three-dimensional ones, variation of the wind field in a lateral direction from the flight path and with time is not included. Thus, during a simulation with these wind models an aircraft moving across the wind field would experience uniform side winds, which is a highly unlikely situation.[5] All the models except one consist of

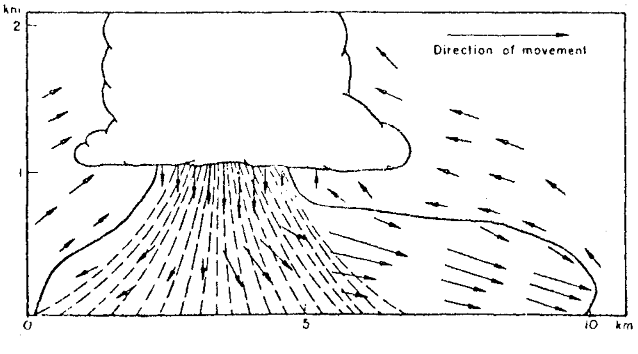

Fig. 1 Section through a thunderstorm in the mature stage.[11]

Received Sept. 9, 1984; revision received Jan. 17, 1985. Copyright © American Institute of Aeronautics and Astronautics, Inc., 1985. All rights reserved.

*Visiting Scholar, on leave from Beijing Institute of Aeronautics and Astronautics, Beijing, China. Member AIAA.

†University Professor Emeritus, Institute for Aerospace Studies. Fellow AIAA.

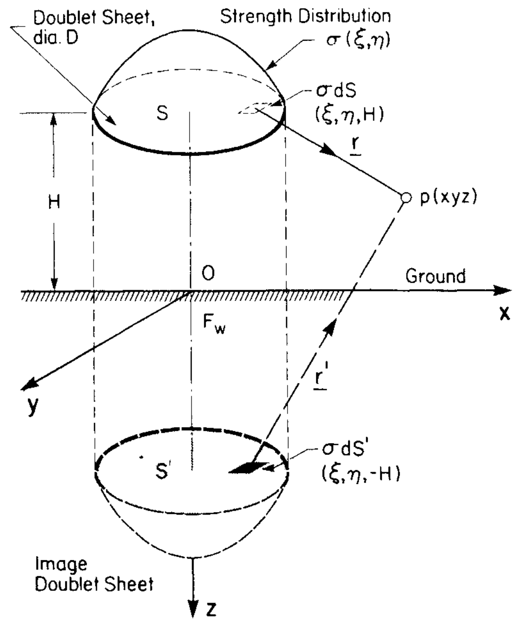

Fig. 2 Three-dimensional doublet-sheet model.

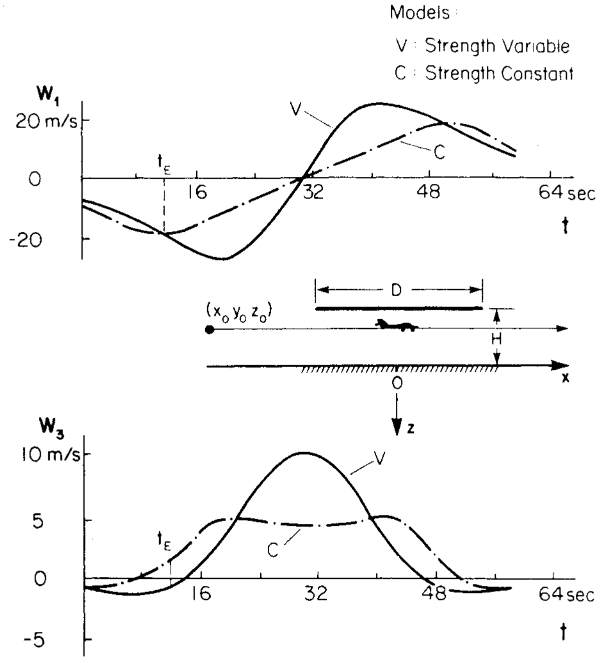

Fig. 3 Comparison of the velocity distributions along a horizontal flight path through microburst for three-dimensional models: ($x_0 = 2190$ m; $h_0 = 200$ m; $y_0 = 0$; $D/H = 3$; $D = 3000$ m).

numerical data in tabulated form. Furthermore, they only include wind variation with height, so that variations with horizontal position are implicit, not explicit. It is clear that the current wind shear models need to be improved.

In Ref. 9, a technique is developed for wind modeling that utilizes the basic fluid-dynamic fields of well-known singularities. Analytical or semianalytical models were investigated, both two- and three-dimensional (axisymmetric). Of these the model based on a circular doublet sheet of variable intensity is recommended as most suitable, and this is the only one described herein.

The similarity of the flowfield to that of a real downburst and the simplicity of implementation should make the proposed model attractive for several applications: 1) analytical investigation of aircraft response to microbursts, 2) developing automatic landing or takeoff systems; 3) providing on-line wind models for flight simulators; and 4) aiding in the certification process for automatic landing systems.

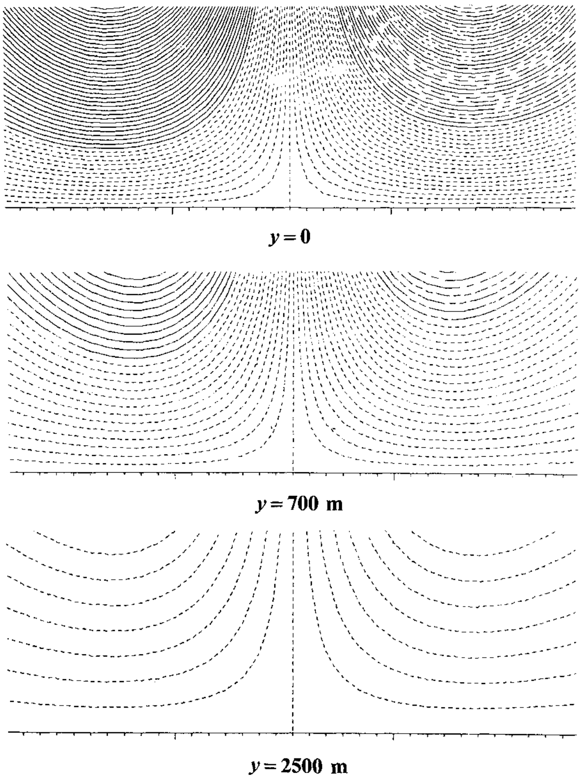
$y = 0$

$y = 700$ m

$y = 2500$ m

Fig. 4 Streamline patterns at different distances from a microburst cell center.

Theory

Considerations in Modeling a Downburst

A number of investigators have proposed specific aeronautical models of wind shear. For application to aircraft response studies, the models used have usually been relatively simple. The main reason for this appears to be that for many purposes a suitably chosen gradient constructed of linear segments will serve just as well for evaluating response as variable winds generated by a complicated, condition-specific atmospheric boundary-layer model. The more complicated models are more expensive to run on a computer and require more computer memory to store, particularly if they are three dimensional. The computer execution time required for calculating a set of wind outputs might be too long for use in an on-line simulator application. An off-line calculation of the wind field can of course be carried out, with the results stored for use in the simulation, using a table look-up technique. This approach lacks the flexibility and adaptability of an on-line calculation and is not the preferred method.

Ideally, what the model should generate is the wind vector as a function of position in a three-dimensional field. Such a model would yield not only the wind at the center of gravity which is the most important feature governing the resultant aerodynamic force for a given airplane attitude, but also the *gradients* of the vertical, horizontal, and lateral wind along the length and span of the airplane. These gradients may provide important inputs to the aerodynamic moments,[10] and hence to the attitude dynamics, during a critical portion of the landing or takeoff. The field produced by the model should, of course, bear a reasonable resemblance to naturally occurring downbursts and should have built-in parameters that enable the scale, velocity distribution, and intensity to be varied.

Varying the size and position of the singularities relative to the ground allows studies to be conducted in which worst cases are sought for particular airplanes or control systems.

The domain of principal interest is that which contains the glide slope or takeoff path, i.e., a region close to the ground. The velocities involved are low compared to the speed of sound, and the ground boundary layer associated with the downburst can be expected to be relatively thin. Thus we take it as reasonable to use an incompressible, inviscid flow in our model. Although evaporative cooling is a dominant element in the physical process that produces the downburst, we have nevertheless included neither variable temperature nor hydrostatic effects in our models. The need to include these should be a subject for future research. Finally, then, we come to a fluid-dynamic model of classical simplicity—an incompressible, inviscid, irrotational flow. Such flows, as is well known, are conveniently generated by distributions of singularities—sources, vortices, and doublets.

Basic Characteristics of the Microburst to be Modeled

Reviewing the work of Byers et al[11] and Fujita[1] leads to a picture of a typical thunderstorm and the associated downburst-outflow as in Fig. 1. Fujita's research results and speculation regarding the phenomena presented in Ref. 1 suggest the existence of narrow downburst cells in some thunderstorms. From the JFK accident records, it was found that three microburst cells could be identified near the approach end of the runway at the time of the B727 accident. Their widths were less than 4.5 km, and they were separated by relatively calm spaces. The bottom of the anvil-like cloud is statistically about one km above the ground. The maximum wind speeds obtained by reconstructing the JFK wind profile were 11.6 m/s vertically and 18 m/s horizontally. As for the flow pattern in a downburst, it is somewhat like that of a jet blowing down against the ground and spreading out radially.

In view of the above, a reasonably realistic model would seem to result from placing a suitable planar distribution of singularities at a height H above the ground, that generates a jet-like downflow of some horizontal extent. To ensure that the ground plane is a stream surface, an image singularity is introduced at $z=-H$.

Development of the Three-Dimensional Model

We now construct a three-dimensional downburst model by using a circular doublet sheet of variable intensity. The reference frame and the key parameters associated with the model are shown in Fig. 2.

A doublet distribution on the surface S at height H of intensity $\sigma(\xi,\eta)$ per unit area, and with axis parallel to z, induces at point $P(x,y,z)$ the velocity components

$$v_x=-\frac{3}{4\pi}\iint_S \sigma(\xi,\eta)\frac{(z-H)(x-\xi)}{r^5}\mathrm{d}\xi\mathrm{d}\eta$$

$$v_y=-\frac{3}{4\pi}\iint_S \sigma(\xi,\eta)\frac{(z-H)(y-\eta)}{r^5}\mathrm{d}\xi\mathrm{d}\eta$$

$$v_z=-\frac{1}{4\pi}\iint_S \sigma(\xi,\eta)\left[\frac{3(z-H)^2}{r^5}-\frac{1}{r^3}\right]\mathrm{d}\xi\mathrm{d}\eta \qquad (1)$$

where

$$r^2=(x-\xi)^2+(y-\eta)^2+(z-H)^2 \qquad (2)$$

In the corresponding expression for the image surface, H is replaced by $-H$, and σ by $-\sigma$.

One method of evaluating these integrals is given in Ref. 10. The result for a doublet sheet with constant strength is given in the Appendix. The corresponding distributions of horizontal and vertical wind components are shown in Fig. 3 (labeled "C").

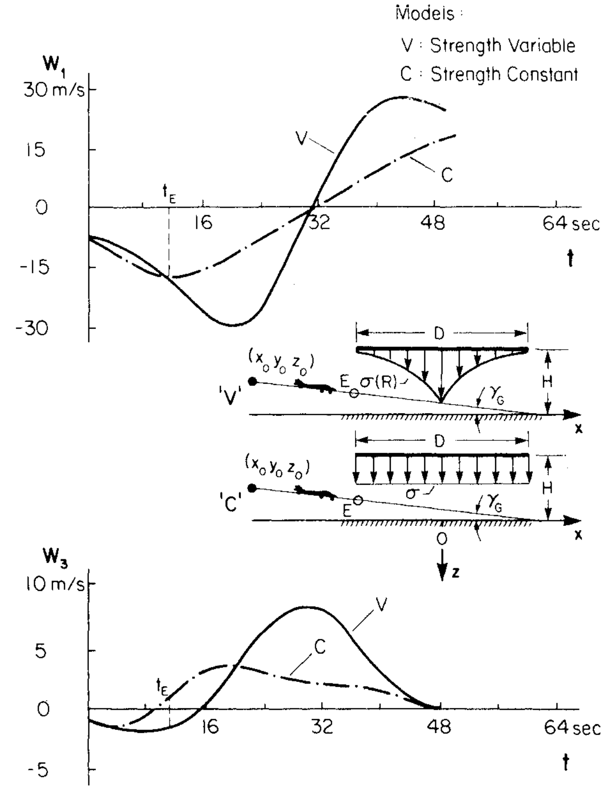

Fig. 5 Comparison of three-dimensional models for different strength distributions: ($x_0=2316$ m; $h_0=200$ m; $y_0=0$; $D/H=3$; $D=3000$ m; $\gamma_G=3$ deg. Comparison condition: $W_1=-18.20$ m/s at "E").

Examining Fig. 3, it was found that the modeled wind field with σ constant was not acceptably close to observed fields. To improve the results, the linear superposition principle of potential flow was employed. A series of uniform concentric doublet sheets of different radius and strength were superimposed approximating a (1-sin) distribution of strength. The resulting flowfield was then reasonable (see Fig. 3, "V"). The number of doublet sheets to be superimposed and the form of the strength distribution functions were chosen by trial-and-error. The number must be chosen to satisfy the requirement of CPU time, and the distribution to meet the requirement of physical realism of the wind field generated. For instance, in our investigation the maximum ratio of vertical to horizontal speed, i.e., $\kappa=W_{3_{\max}}/W_{1_{\max}}$, was taken as a criterion, and the CPU time on an IBM 370-type computer for a run to generate a wind vector was limited to less than 0.03 s. The following strength distribution function is recommended in this paper:‡

$$\sigma(R)=\sigma_m[1-\sin(R/R_0)] \qquad (3)$$

This can be approximated by a superposition of constant-strength sheets as follows:

$$\sigma(R)=\sum_{i=1}^{N}\sigma_i \qquad (4a)$$

---

‡In Ref. 10 Eq. 2-10 for the three-dimensional case, and the corresponding equation for the two-dimensional case, describe a dome-shaped distribution of intensity. Actually, the computed results are for a tent-shaped (1-sin) distribution function, as given in this paper. Also, the program listing attached in Ref. 10 was not properly connected.

where

$$\sigma_i = k \cos(\pi/2)(R_i/R_0) \tag{4b}$$

and

$$R_0 = R_0 - i\Delta R \tag{4c}$$

k = a constant, chosen to generate the desired downburst intensity $= \sigma_m/N$

$$\Delta R = R_0/N$$

Then the speeds at point $P(x,y,z)$ induced by the equivalent doublet sheet with variable strength are as follows:

$$v_x = \sum_{i=1}^{N} \sigma_i v_{xo_i} \tag{5}$$

$$v_y = \sum_{i=1}^{N} \sigma_i v_{yo_i} \tag{6}$$

$$v_z = \sum_{i=1}^{N} \sigma_i v_{zo_i} \tag{7}$$

Figure 4 gives an example of the flowfield obtained by the above method. (For an axial-symmetric flow, the Stokes stream function is obtained in the usual way, as shown in Ref. 12.) Figure 3 also shows how the vertical and horizontal velocities vary along a horizontal line 200 m above ground, where the doublet sheet is at 1000 m altitude. These velocity distributions are in reasonable accord with physical reality.

The wind profiles along a 3 deg glide slope for the models of variable doublet strengths are plotted in Fig. 5. The glide slopes are so chosen that the "touchdown-point" is directly under the far edge of the doublet sheet. The time scale corresponds to a flight speed of 73.1 m/s. It is found that the ver-

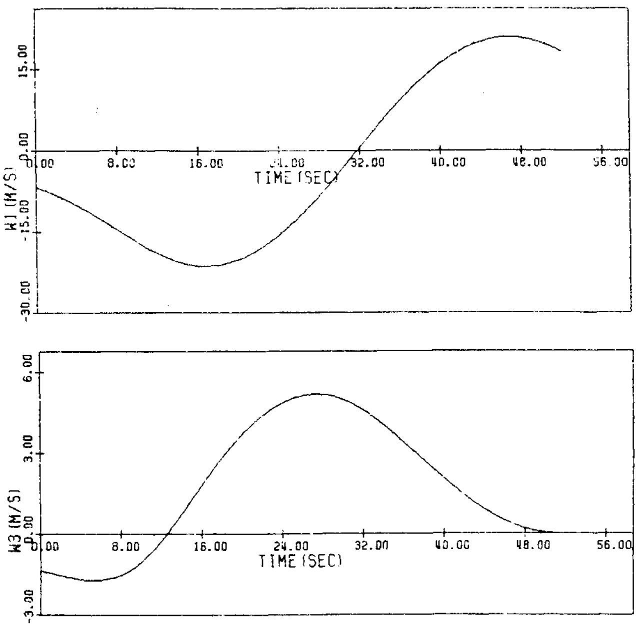

Fig. 6 Wind variation along a 3 deg glide slope ($x_{TD} = D/2$; $y = 0$; $h_0 = 200$ m; W_2 is null).

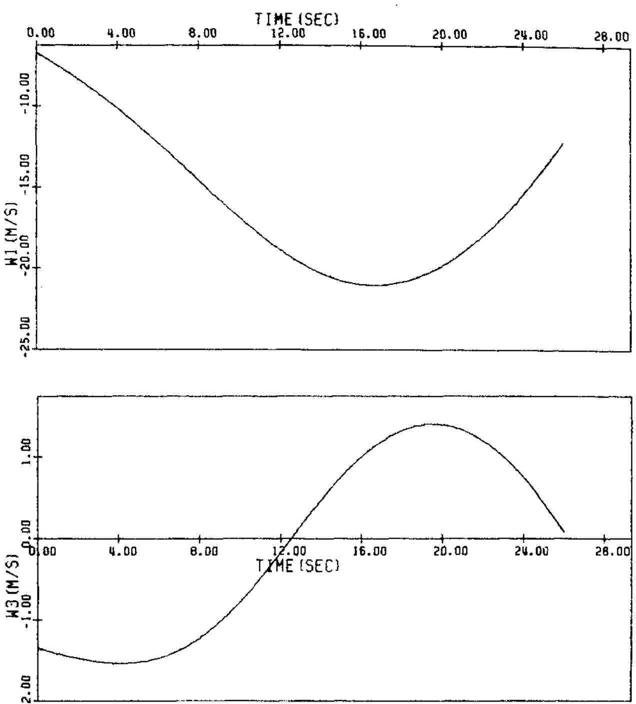

Fig. 7 Wind variation along a 6 deg glide slope ($x_{TD} = 0$; $y = 0$; $h_0 = 200$ m; W_2 is null).

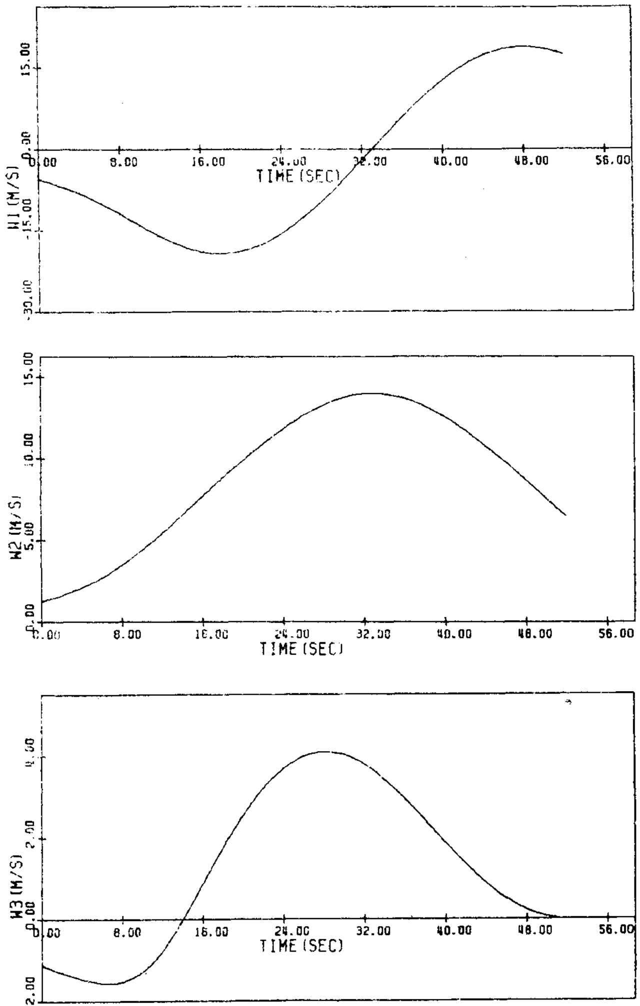

Fig. 8 Wind variation along a 3 deg glide slope ($x_{TD} = D/2$; $y = D/4$; $h_0 = 200$ m).

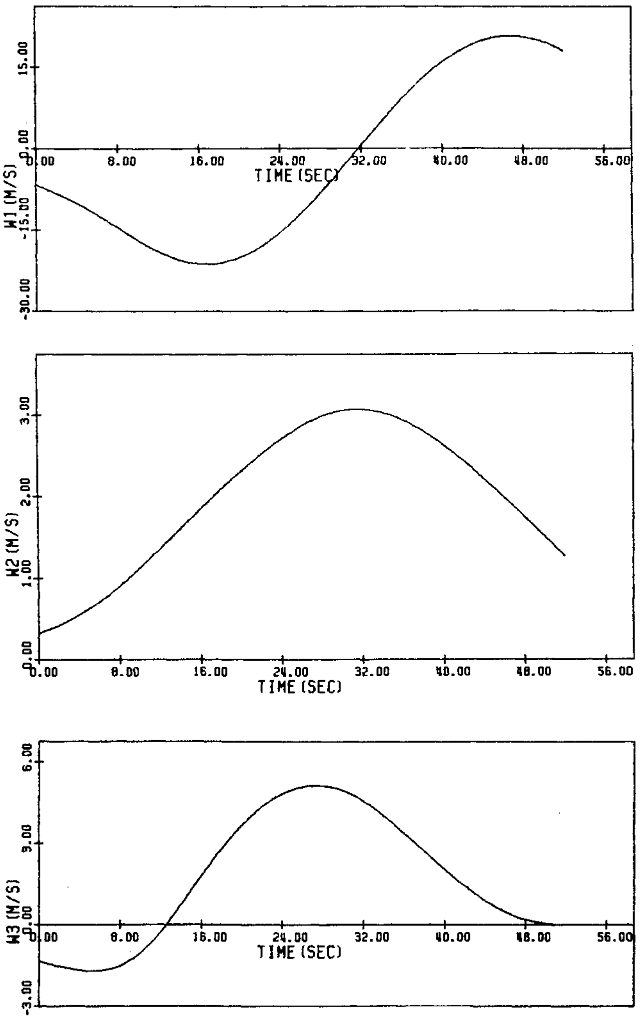

Fig. 9 Wind variation along a 3 deg glide slope ($x_{TD} = 0.471D$; $y = 500$ m; $h_0 = 200$ m).

tical and horizontal winds have an oscillatory character. The period for the case shown is roughly 40 s which is close to the phugoid period of B747-type aircraft at landing speed. In particular, the ratio of $W_{3_{\max}}/W_{1_{\max}}$ for this model is similar to that of a real microburst.

Application to Flight Simulation and Wind Profile Demonstration

The model developed in this investigation can, of course, be readily applied to computations of flight path on a digital computer. Application to on-line generation of the windfield for human-piloted simulators additionally requires that the cycle time be sufficiently small. On the University of Toronto IBM 370 this time for the three-dimensional model with (1-sin) distribution and with $N = 3$, using a program not considered to be optimum, is less than 0.015 s, so the wind field could be updated about 67 times per s. This repetition rate would of course be lower on a less powerful computer. With a good computer and optimum programming, the repetition time required for the overall simulation (10 to 30 updates per s) could be achieved with the three-dimensional model.

Two sets of parameters influence the wind time-history experienced by an airplane during a landing or takeoff. One set is related to the model itself, i.e., $\{H, D, \sigma(r)\}$. Another set is related to the flight path, for example, during a landing, the glide-slope angle, the location of the touchdown point relative to the doublet sheet, and the lateral position of the glide slope relative to the doublet sheet (coordinate y). A very strong parameter, insofar as the ratio of horizontal to vertical wind is concerned, is the shape of the distribution $\sigma(r)$. We found a (1-sin) law to give results like those obtained in reconstructed accident profiles. Stronger downdrafts can be obtained by using distributions more highly peaked at the center.

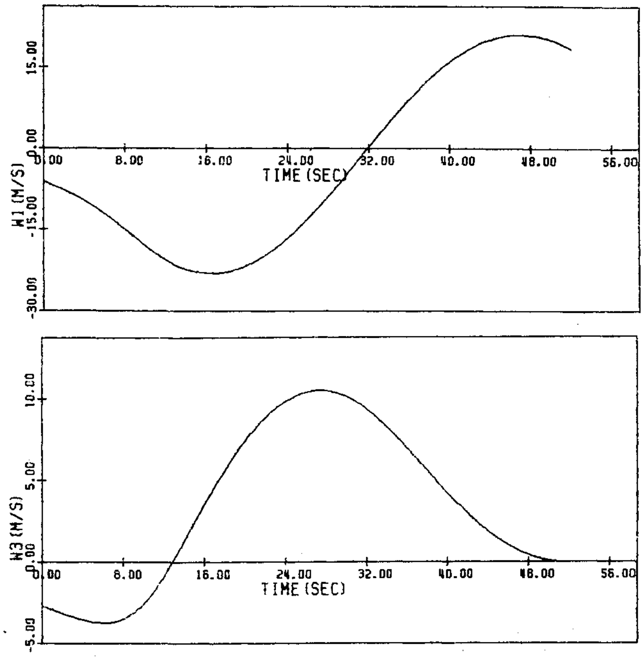

Fig. 10 Wind variation along a 6 deg glide slope ($x_{TD} = D/2$; $y = 0$; $h_0 = 400$ m).

By way of example, we show the effect of varying the glide slope steepness and location on time histories of W_1, W_2, and W_3 for an approach speed of about 73 m/s. These are shown in Figs. 6-10. The figures show that the wind history experienced by the airplane varies appreciably from case to case, especially when the presence of W_2 (side wind) is considered in the cases where $y \neq 0$. The variability of these time-histories makes this a useful model for human-piloted simulations, in that exact repetitions can easily be avoided.

We see that the side wind W_2 varies strongly with the position of the glide slope relative to the center of the doublet sheet. Actually, as the distance from the center increases, W_2 increases at first but then decreases. The strongest side wind occurs at a lateral distance of about $D/4$ from the center; and its magnitude is of the same order as the head wind, as shown in Fig. 8. Comparing Figs. 6 and 10, which are both for a touchdown point under the far edge of the downburst cell, we note that the profiles are very similar in shape and magnitude, but that the 6 deg glide-slope case encounters a slightly stronger downburst. This implies that the wind profile encountered depends mainly upon the touchdown position. A comparison of two touchdown positions is provided by Figs. 7 and 10. The flight path that penetrates less into the downburst (see Fig. 7) experiences only a head wind and very little vertical wind.

Concluding Remarks

A microburst model, synthesized using distributed singularities, has been implemented and evaluated on a digital computer. The model is reasonably representative of the wind field near the ground during the mature phase of a thunderstorm downburst. It shows general agreement with other work for both models derived from wind measurements and accident reconstructions. The advantage of the present technique over prerecorded deterministic models is that it produces a three-dimensional wind input that depends on the flight path and has three adjustable parameters. The proposed model is realistic and relatively easy to implement for flight simulation, in particular for on-line wind shear generation.

It should be noted that the model permits the representation of lateral inputs (e.g., W_2 and rolling gusts $\partial W_3/\partial y$), so that pilot workload in manual flight is made more realistic.

It is also noted that for the microburst cell with 3 ~ 4 km diameter, the horizontal and vertical components along a 3 deg glide slope have an oscillatory character, the period of which is close to the phugoid mode of large jet transports at landing speed.

Variations in the model for any given case are easily generated by changing the basic parameters H, D, and σ_m. It is also easy to add an additional uniform horizontal wind to generate a "biased" downflow.

Experimental data suggest that there may be a ring vortex close to the ground at the extremity of the outflow. Although we have not added this feature to the present model, it would clearly be feasible to do so using the same basic mathematics.

Appendix: Complete Formulas for Three Wind Speed Components Generated by a Uniform Strength Doublet Sheet of Unit Strength

Headwind

$$
\begin{aligned}
V_{x_0}=\frac{3}{4\pi}\Bigg[&(z-H)\int_{-R}^{R}(x\text{-}\xi)\left\{\frac{2(y-\sqrt{R^2-\xi^2})^3+3(y-\sqrt{R^2-\xi^2})[(x-\xi)^2+(z-\zeta)^2]}{3[(x-\xi)^2+(z-\zeta)^2]^2[(x-\xi)^2+(z-\zeta)^2+(y-\sqrt{R^2-\xi^2})^2]^{3/2}}\right.\\
&\left.-\frac{2(y+\sqrt{R^2-\xi^2})^2+3(y+\sqrt{R^2-\xi^2})[(x-\xi)^2+(z-\zeta)^2]}{3[(x-\xi)^2+(z-\zeta)^2]^2[(x-\xi)^2+(z-\zeta)^2+(y+\sqrt{R^2-\xi^2})^2]^{3/2}}\right\}\mathrm{d}\xi\\
&-(z-H)\int_{-R}^{R}(x-\xi)\left\{\frac{2(y-\sqrt{R^2-\xi^2})^3+3(y-\sqrt{R^2-\xi^2})[(x-\xi)^2+(z+\zeta)^2]}{3[(x-\xi)^2+(z+\zeta)^2]^2[(x-\xi)^2+(z+\zeta)^2+(y-\sqrt{R^2-\xi^2})^2]^{3/2}}\right.\\
&\left.-\frac{2(y+\sqrt{R^2-\xi^2})^2+3(y+\sqrt{R^2-\xi^2})[(x-\xi)^2+(z+\zeta)^2]}{3[(x-\xi)^2+(z+\zeta)^2]^2[(x-\xi)^2+(z+\zeta)^2+(y+\sqrt{R^2-\xi^2})^2]^{3/2}}\right\}\mathrm{d}\xi\Bigg]
\end{aligned}
\tag{A1}
$$

Sidewind

$$
\begin{aligned}
V_{y_0}=\frac{3}{4\pi}\Bigg[&(z-H)\int_{-R}^{R}(y-\eta)\left\{\frac{2(x-\sqrt{R^2-\eta^2})^3+3(y-\sqrt{R^2-\eta^2})[(y-\eta)^2+(z-\zeta)^2]}{3[(y-\eta)^2+(z-\zeta)^2]^2[(y-\eta)^2+(z-\zeta)^2+(x-\sqrt{R^2-\eta^2})^2]^{3/2}}\right.\\
&\left.-\frac{2(x+\sqrt{R^2-\eta^2})^2+3(x+\sqrt{R^2-\eta^2})[(y-\eta)^2+(z-\zeta)^2]}{3[(y-\eta)^2+(z-\zeta)^2]^2[(y-\eta)^2+(z-\zeta)^2+(x+\sqrt{R^2-\eta^2})^2]^{3/2}}\right\}\mathrm{d}\eta\\
&-(z+H)\int_{-R}^{R}(y-\eta)\left\{\frac{2(x-\sqrt{R^2-\eta^2})^3+3(x-\sqrt{R^2-\eta^2})[(y-\eta)^2+(z+\zeta)^2]}{3[(y-\eta)^2+(z+\zeta)^2]^2[(y-\eta)^2+(z+\zeta)^2+(x-\sqrt{R^2-\eta^2})^2]^{3/2}}\right.\\
&\left.-\frac{2(x+\sqrt{R^2-\eta^2})^2+3(x+\sqrt{R^2-\eta^2})[(y-\eta^2)^2+(z-\zeta)^2]}{3[(y-\eta)^2+(z-\zeta)^2]^2[(y-\eta)^2+(z-\zeta)^2+(x+\sqrt{R^2-\eta^2})^2]^{3/2}}\right\}\mathrm{d}\eta\Bigg]
\end{aligned}
\tag{A2}
$$

Vertical Wind

$$
\begin{aligned}
V_{z_0}=\frac{1}{4\pi}\Bigg[&3(z-H)^2\int_{-R}^{R}\left\{\frac{2(y-\sqrt{R^2-\xi^2})^3+3(y-\sqrt{R^2-\xi^2})[(x-\xi)^2+(z-\zeta)^2]}{3[(x-\xi)^2+(z-\zeta)^2]^2[(x-\xi)^2+(z-\zeta)^2+(y-\sqrt{R^2-\xi^2})^2]^{3/2}}\right.\\
&\left.-\frac{2(y+\sqrt{R^2-\xi^2})^3+3(y-\sqrt{R^2-\xi^2})[(x-\xi)^2-(z-\zeta)^2]}{3[(x-\xi)^2+(z-\zeta)^2]^2[(x-\xi)^2+(z-\zeta)^2+(y+\sqrt{R^2-\xi^2})^2]^{3/2}}\right\}\mathrm{d}\xi\\
&-3(z+H)^2\int_{-R}^{R}\left\{\frac{2(y-\sqrt{R^2-\xi^2})^3-3(y-\sqrt{R^2-\xi^2})[(x-\xi)^2+(z+\zeta)^2]}{3[(x-\xi)^2+(z-\zeta)^2]^2[(x-\xi)^2+(z+\zeta)^2+(y-\sqrt{R^2-\xi^2})^2]^{3/2}}\right.\\
&\left.-\frac{2(y+\sqrt{R^2-\xi^2})^3+3(y+\sqrt{R^2-\xi^2})[(x-\xi)^2+(z+\zeta)^2]}{3[(x-\xi)^2+(z+\zeta)^2]^2[(x-\xi)^2+(z+\zeta)^2+(y+\sqrt{R^2-\xi^2})^2]^{3/2}}\right\}\mathrm{d}\xi\\
&-\int_{-R}^{R}\left\{\frac{y-\sqrt{R^2-\xi^2}}{[(x-\xi)^2+(z-\zeta)^2]\sqrt{(x-\xi^2)+(z-\zeta)^2+(y-\sqrt{R^2-\xi^2})^2}}\right.\\
&\left.-\frac{y+\sqrt{R^2-\xi^2}}{[(x-\xi)^2+(z-\zeta)^2]\sqrt{(x-\xi^2)+(z-\zeta)^2+(y+\sqrt{R^2-\xi^2})^2}}\right\}\mathrm{d}\xi\\
&+\int_{-R}^{R}\left\{\frac{y-\sqrt{R^2-\xi^2}}{[(x-\xi)^2+(z+\zeta)^2]\sqrt{(x-\xi^2)+(z+\zeta)^2-(y+\sqrt{R^2-\xi^2})^2}}\right.\\
&\left.-\frac{y+\sqrt{R^2-\xi^2}}{[(x-\xi)^2+(z+\zeta)^2]\sqrt{(x-\xi^2)+(z+\zeta)^2+(y+\sqrt{R^2-\xi^2})^2}}\right\}\mathrm{d}\xi\Bigg]
\end{aligned}
\tag{A3}
$$

References

[1] Fujita, T. T., "Spearhead Echo and Downburst Near the Approach End of a John F. Kennedy Airport Runway, New York City," SMRP Research Paper 137, March 1976.

[2] Wilson, J. and Fujita, T. T., "The Joint Airport Weather Studies Project," Bulletin of the American Meteorological Society, Vol. 63, 1982, pp. 15-22.

[3] Frost, W., Chang, H. P., McCarthy, J., and Elmore K., "Simulated Flight Through JAWS Wind Shear: In-Depth Analysis Results," AIAA Paper 84-0276, Jan. 1984.

[4] Psiaki, M. and Stengel, R. F., "Analysis of Aircraft Control Strategies for Microburst Encounter," AIAA Paper 84-0238, Jan. 1984.

[5] Frost, W., "Flight in Low-Level Wind Shear," NASA CR-3678, 1983.

[6] Williamson, G. G., Lewellen, W. S., and Teske, M. E., "Model Predictions of Wind and Turbulence Profiles Associated with an Ensemble of Aircraft Accidents," NASA CR-2884, July 1977.

[7] Goff, C., Lee, J. T., and Brandes, E. A., "Gust Front Analytical Study," U.S. Department of Transportation, Washington, D.C., FAA Rept. FAA-RD-77-19, 1977.

[8] Foy, W. H., "Airborne Aids for Coping with Low-Level Wind Shear," U.S. Department of Transportation, Washington, D.C., Rept. FAA-RD-79-117, 1979.

[9] Zhu, Shangxiang and Etkin, B., "Fluid-Dynamic Model of a Downburst," University of Toronto, Institute for Aerospace Studies, Toronto, Canada, UTIAS Rept. 271, April 1983.

[10] Etkin, B., "The Turbulent Wind and Its Effect on Flight" (AIAA Wright Brothers Lecture), University of Toronto, Institute of Aerospace Studies Review No. 44, Aug. 1980.

[11] Byers, M. R. and Braham, R. R. Jr., "The Thunderstorm," Government Printing Office, Washington, D.C., 1949.

[12] Batchelor, G. K., *An Introduction to Fluid Dynamics*, University of Cambridge Press, Cambridge, England, UK, 1967.

From the AIAA Progress in Astronautics and Aeronautics Series . . .

COMBUSTION EXPERIMENTS IN A ZERO-GRAVITY LABORATORY—v. 73

Edited by Thomas H. Cochran, NASA Lewis Research Center

Scientists throughout the world are eagerly awaiting the new opportunities for scientific research that will be available with the advent of the U.S. Space Shuttle. One of the many types of payloads envisioned for placement in earth orbit is a space laboratory which would be carried into space by the Orbiter and equipped for carrying out selected scientific experiments. Testing would be conducted by trained scientist-astronauts on board in cooperation with research scientists on the ground who would have conceived and planned the experiments. The U.S. National Aeronautics and Space Administration (NASA) plans to invite the scientific community on a broad national and international scale to participate in utilizing Spacelab for scientific research. Described in this volume are some of the basic experiments in combustion which are being considered for eventual study in Spacelab. Similar initial planning is underway under NASA sponsorship in other fields—fluid mechanics, materials science, large structures, etc. It is the intention of AIAA, in publishing this volume on combustion-in-zero-gravity, to stimulate, by illustrative example, new thought on kinds of basic experiments which might be usefully performed in the unique environment to be provided by Spacelab, i.e., long-term zero gravity, unimpeded solar radiation, ultra-high vacuum, fast pump-out rates, intense far-ultraviolet radiation, very clear optical conditions, unlimited outside dimensions, etc. It is our hope that the volume will be studied by potential investigators in many fields, not only combustion science, to see what new ideas may emerge in both fundamental and applied science, and to take advantage of the new laboratory possibilities.

Published in 1981,280 pp., 6×9, illus., $25.00 Mem., $39.00 List

TO ORDER WRITE: Publications Order Dept., AIAA, 1633 Broadway, New York, N.Y. 10019